

HEP'99 # 6_360

DELPHI 99-63 CONF 250

Submitted to Pa 6

15 June 1999

P1 6

Measurement of Trilinear Gauge Boson Couplings in e^+e^- Collisions at 189 GeV

Preliminary

DELPHI Collaboration

OPEN-99-408
15/06/1999



Paper submitted to the HEP'99 Conference
Tampere, Finland, July 15-21

Measurement of Trilinear Gauge Boson Couplings in e^+e^- Collisions at 189 GeV

T.J.V. Bowcock¹, C. DeClercq², G. Fanourakis³, D. Fassouliotis³, D. Gelé⁴,
B. Golob⁵, B. Kersevan⁵, A. Kinzig¹, V. Kostioukhine⁶, J. Libby⁷, A. Leisos³,
N. Mastroiannopoulos³, C. Matteuzzi⁸, M. McCubbin¹, M. Nassiakou³,
G. Orazi⁴, U. Parzefall¹, H.T. Phillips⁹, R.L. Sekulin⁹, F. Terranova⁸,
S. Tzamarias³, A. Van Lysebetten², O. Yushchenko⁶

¹ Department of Physics, University of Liverpool, P.O. Box 147, Liverpool L69 3BX, UK

² IIHE-Institut Universitaire des Hautes Energies, Pleinlaan 2, B-1050 Brussels, Belgium

³ Institute of Nuclear Physics, N.C.S.R. Demokritos, P.O. Box 60228, GR-15310 Athens, Greece

⁴ Institut de Recherches Subatomiques, B.P. 20 CRO, F-67037 Strasbourg Cedex, France

⁵ Univerza v Ljubljani, Institut Josef Stefan, Jamova 39, P.O.B 3000, SI-1001 Ljubljana, Slovenia

⁶ Inst. for High Energy Physics, Serpukhov P.O. Box 35, Protvino, (Moscow Region), Russian Federation

⁷ Department of Physics, University of Oxford, Keble Road, Oxford OX1 3RH, UK

⁸ Dipartimento di Fisica, Università di Milano and INFN, Via Celoria 16, I-20133 Milan, Italy

⁹ Rutherford Appleton Laboratory, Chilton, Didcot OX11 0QX, UK

Abstract

Preliminary measurements of the trilinear gauge boson couplings $WW\gamma$ and WWZ are presented from data taken by DELPHI in 1998 at an energy of 189 GeV and combined with available DELPHI data at lower energies. Values are determined for Δg_1^Z and $\Delta\kappa_\gamma$, the differences of the WWZ charge coupling and of the $WW\gamma$ dipole couplings from their Standard Model values, and for λ_γ , the $WW\gamma$ quadrupole coupling. The study uses data from the final states $jj\ell\nu$, $jjjj$, $\ell^+\ell^-X$, ℓX , jjX and γX , where j represents a quark jet, ℓ an identified lepton and X missing four-momentum. Data from the jjX and $\ell^+\ell^-X$ topologies are also used to derive values for the ZZV couplings f_4^{ZZV} and f_5^{ZZV} ($V \equiv \gamma, Z$) defined by Hagiwara *et al.* [1]. The observations are consistent with the predictions of the Standard Model.

1 Introduction

This study of trilinear gauge boson couplings uses data from the final states $jj\ell\nu$, $jjjj$, $\ell^+\ell^-X$, ℓX , jjX and γX (where j represents a quark jet, ℓ an identified lepton and X missing four-momentum) taken by the DELPHI detector at LEP in 1998 at a centre-of-mass energy of 189 GeV. The data are used to determine values of three coupling parameters at the WWV vertex (with $V \equiv \gamma, Z$): Δg_1^Z , the difference between the value of the overall WWZ coupling strength and its Standard Model prediction; $\Delta\kappa_\gamma$, the difference between the value of the dipole coupling, κ_γ , and its Standard Model value; and λ_γ , the $WW\gamma$ quadrupole coupling parameter. In addition, the samples collected in the topologies jjX and $\ell^+\ell^-X$ contain contributions from the four-fermion final states $q\bar{q}\nu\bar{\nu}$ and $\ell^+\ell^-\nu\bar{\nu}$ which can be produced by processes involving ZZZ and $ZZ\gamma$ couplings. Contributions from these vertices, which are forbidden in the Standard Model, are described by the parameters f_4^{ZZV} and f_5^{ZZV} ($V \equiv \gamma, Z$) defined by Hagiwara *et al.* [1].

In the evaluation of the WWV couplings, a model has been assumed [2] in which contributions to the effective WWV Lagrangian from operators describing possible new physics beyond the Standard Model are restricted to those which are CP -conserving, are of lowest dimension (≤ 6), satisfy $SU(2) \times U(1)$ invariance and have not been excluded by previous measurements. This leads to possible contributions from three operators, $\mathcal{L}_{W\phi}$, $\mathcal{L}_{B\phi}$ and \mathcal{L}_W , and hence to relations between the permitted values of the $WW\gamma$ and WWZ couplings: $\Delta\kappa_Z = \Delta g_1^Z - \frac{s_w^2}{c_w^2}\Delta\kappa_\gamma$, $\lambda_Z = \lambda_\gamma$, where s_w and c_w are the sine and cosine of the electroweak mixing angle. The parameters we determine are related to possible contributions $\alpha_{W\phi}$, $\alpha_{B\phi}$ and α_W from the three operators given above by: $\Delta g_1^Z = \alpha_{W\phi}/c_w^2$, $\Delta\kappa_\gamma = \alpha_{W\phi} + \alpha_{B\phi}$, and $\lambda_\gamma = \alpha_W$.

The WWV coupling arises in WW production through the diagrams involving s -channel exchange of Z or γ , shown in figure 1a. We study this reaction in the final states $jj\ell\nu$, where one W decays into quarks and the other into leptons, $jjjj$, where both W s decay into quarks, and $\ell^+\ell^-X$, where both W s decay leptonically.

In single W production, the dominant amplitude involving a trilinear gauge coupling arises from the radiation of a virtual photon from the incident electron or positron, interacting with a virtual W radiated from the other incident particle (figure 1b). This process, involving a $WW\gamma$ coupling, contributes significantly in the kinematic region where a final state electron or positron is emitted at small angle to the beam and is thus likely to remain undetected in the beam pipe. The decay modes of the W give rise to two final states: that with two jets and missing energy (jjX), and that containing only a single lepton coming from the interaction point and no other track in the detector (ℓX).

The trilinear $WW\gamma$ vertex also occurs in the reaction $e^+e^- \rightarrow \nu\nu\gamma$ in the diagram in which the incoming electron and positron each radiate a virtual W at an $e\nu W$ vertex and these two fuse to produce an outgoing photon (figure 1c). In this process, which leads to a final state, γX , consisting of a single detected photon, the $WW\gamma$ coupling is studied completely independently of the WWZ coupling, as no WWZ vertex is involved. In the Standard Model, the dominant mechanism for production of this final state is via the reaction $e^+e^- \rightarrow Z\gamma$, with the photon produced by initial state radiation and with the Z decaying into $\nu\bar{\nu}$.

Diagrams involving trilinear ZZV vertices and giving rise to the four-fermion final states $q\bar{q}\nu\bar{\nu}$ and $\ell^+\ell^-\nu\bar{\nu}$ are shown in figures 1d and 1e. We study two possible couplings involved in the Lorentz-invariant description of these vertices; one of them, f_4^{ZZV} , is

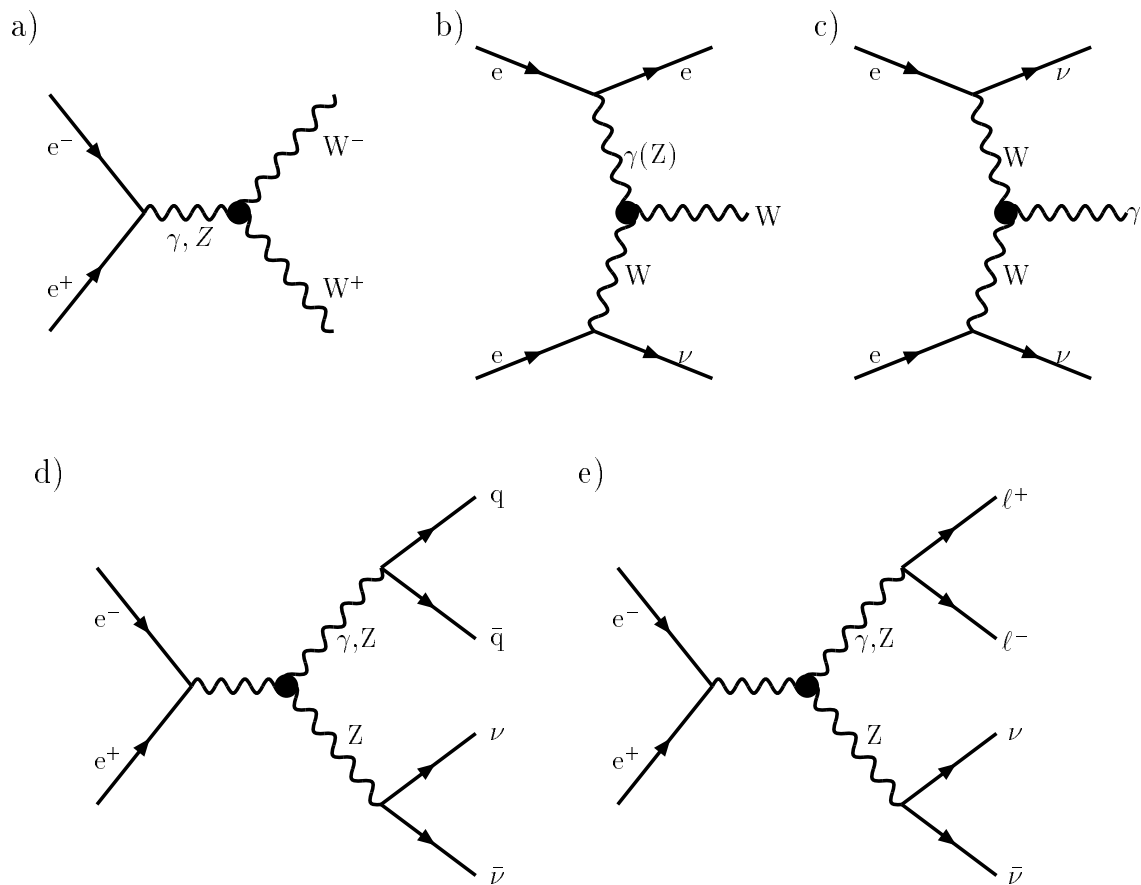


Figure 1: Diagrams with trilinear gauge boson couplings contributing to the processes studied in this paper: a) $e^+e^- \rightarrow W^+W^-$, b) $e^+e^- \rightarrow W e \nu$, c) $e^+e^- \rightarrow \nu \nu \gamma$, d) $e^+e^- \rightarrow q \bar{q} \nu \bar{\nu}$, e) $e^+e^- \rightarrow \ell^+ \ell^- \nu \bar{\nu}$.

CP -odd and the other, f_5^{ZZV} , is C - and P -odd.

The next section of this paper describes the selection of events from the data and the simulation of the various channels involved in the analysis, and section 3 describes the methods used in the determination of coupling parameters. In section 4 the results from different channels are presented and combined with previously published DELPHI results [3, 4] to give overall values for the coupling parameters. A summary is given in section 5.

2 Event selection and simulation

In 1998 DELPHI recorded a total integrated luminosity of 155 pb^{-1} at an average centre-of-mass energy of 189 GeV. We describe here the main features of the selection of events in the final state topologies $jj\ell\nu$, $jjjj$, $\ell^+\ell^-X$, ℓX , jjX and γX , defined in the previous section. A detailed description of the DELPHI detector may be found in [5], which includes descriptions of the main components of the detector used in this study, namely,

the trigger system, the luminosity monitor, the tracking system in the barrel and forward regions, the muon detectors, the electromagnetic calorimeters and the hermeticity counters. The definition of the criteria imposed for track selection and lepton identification and a description of the luminosity measurement are described in [6].

Selection of events in the $jj\ell\nu$ topology:

Events in the $jj\ell\nu$ topology are characterized by two hadronic jets, a lepton and missing momentum resulting from the neutrino. The lepton may be an electron or muon (coming either from W decay or from the cascade decay $W \rightarrow \tau \dots \rightarrow \ell \dots$) or, in the case of τ decays, it might give rise to a low multiplicity jet. The major backgrounds come from $q\bar{q}(\gamma)$ production and from four-fermion final states containing two quarks and two leptons of the same flavour.

The selection procedure followed closely that used in our analysis of data at 183 GeV, with only certain kinematic cuts changed in the selection of electron candidates.

Events with several hadrons were selected by requiring 5 or more charged particles and total energy of charged particles recorded in the detector exceeding 15% of the centre-of-mass energy. In the selection of $jj\mu\nu$ and $jj\ell\nu$ events, the candidate lepton was assumed to be the most energetic charged particle in the event, while for $jj\tau\nu$ events the lepton candidates were constructed by looking for an isolated e or μ or a low multiplicity jet.

All particles except that corresponding to the candidate lepton were forced into two jets using the LUCLUS algorithm [7]. To remove $\gamma\gamma$ interactions and poorly reconstructed events each quark jet was required to have no less than 4 particles, at least one being charged, and the invariant mass of the two jets was required to exceed $30 \text{ GeV}/c^2$. Furthermore, events were required to have missing momentum above $10 \text{ GeV}/c$ and no detected isolated photon with energy above 40 GeV.

Events with a candidate muon in the final state were accepted if the momentum of the candidate exceeded $25 \text{ GeV}/c$ (or $5 \text{ GeV}/c$ for τ candidates decaying into muons) and if the isolation angle of the candidate (defined as the angle between the muon and the nearest particle with momentum above $1 \text{ GeV}/c$) exceeded a value between 8° and 20° , depending on the quality of the muon identification. Non-isolated particles which were tagged as muons were also considered as candidates if the missing momentum of the event exceeded $20 \text{ GeV}/c$ and if the polar angle of the missing momentum, $\theta_{p_{miss}}$, satisfied $|\cos \theta_{p_{miss}}| < 0.95$.

The selection of events with an electron in the final state followed a similar procedure: charged particles with energy deposition in the electromagnetic calorimeters of at least 20 GeV were accepted as candidates. For tau candidates decaying into electrons, the energy deposition was required to exceed 5 GeV and to match the momentum within $\pm 20\%$. The component of the missing momentum transverse to the beam axis was required to be greater than $15 \text{ GeV}/c$ and the angle between the candidate and the missing momentum to exceed 60° . The isolation angle of the candidate with respect to the nearest charged particle of momentum greater than $1 \text{ GeV}/c$ was required to exceed 5° for electrons observed in the barrel region of the detector, or 10° for electrons in the forward region.

In order to increase the efficiency of the selection, cases where the candidate was not identified as a lepton were also treated. Kinematic requirements in this case were tighter, accepting only events satisfying $|\cos \theta_{p_{miss}}| < 0.95$ (or < 0.87 for events where the lepton

was an electron candidate). In addition, events were required to satisfy the condition $\sqrt{s'} < \sqrt{s} - 5$ GeV, where $\sqrt{s'}$ is an estimate of the effective collision energy in the (background) $q\bar{q}(\gamma)$ final state after initial state radiation [8].

Four-fermion backgrounds ($q\bar{q}\ell\ell$) were reduced by applying an additional cut to events in which a second lepton of the same flavour and with charge opposite to that of the candidate was found. The event was rejected if the second lepton had momentum above 5 GeV/ c and isolation angle with respect to all other particles except the candidate greater than 15°.

In the selection of $jj\tau\nu$ events with a τ decaying into hadrons, events were accepted if, using LUCLUS with $d_{join} = 3$ GeV/ c , they were found to have at least 3 jets, and if both the missing energy and the transverse energy exceeded 40 GeV. The tau candidate jet was required to have total multiplicity ≤ 5 , only one charged particle, total momentum above 10 GeV/ c and to be isolated from other jets by more than 25°. In addition, in order to reduce the fully hadronic WW background, the event was rejected if it had four or more jets reconstructed with $d_{join} = 10$ GeV/ c .

A 3-constraint kinematic fit was then performed on candidate e and μ events, imposing energy and momentum conservation and the nominal W mass on both W s. For candidate τ events, a 2-constraint fit was performed, in which the τ momentum was left unconstrained, while its direction was taken to be that of its detected decay products.

The efficiency for the selection of $jj\ell\nu$ events was evaluated using fully simulated events to be 80%, 59% and 32% for muon, electron and tau events, respectively. Using data taken only when all essential components of the detector were operational, corresponding to an integrated luminosity of 149 pb $^{-1}$, 263 muon, 211 electron and 152 tau candidate events were selected. A background contamination of 0.226 pb was estimated, of which 58% came from the $q\bar{q}(\gamma)$ final state, 22% from Ze^+e^- , 13% from ZZ and $Z\gamma^*$ production, and small contributions from non-semileptonic WW events and other sources.

Selection of events in the $jjjj$ topology:

The selection of events in the fully hadronic topology followed closely that used in our analysis of data at 183 GeV, with only small changes in the values of kinematic cuts.

All detected particles were first clustered into jets using LUCLUS with $d_{join} = 5.5$ GeV/ c . Events were accepted if they had at least four jets, with at least four particles per jet. Background from $Z\gamma$ events was suppressed by imposing the condition $\sqrt{s'} > 130$ GeV. Events were then forced into a 4-jet configuration and a 4-constraint fit performed, requiring conservation of four-momentum. Then, in order to suppress the dominant background, which arises from the $q\bar{q}\gamma$ final state, the condition $D > 0.0055$ GeV $^{-1}$ was imposed, with $D = \frac{E_{min}\theta_{min}}{E_{max}} / (E_{max} - E_{min})$; E_{min} and E_{max} are the energies of the reconstructed jets with minimum and maximum energy and θ_{min} is the minimum interjet angle. A further fit was then performed on surviving events, imposing four-momentum conservation and requiring the masses of the two reconstructed W s to be equal. The fit was applied to all three possible pairings of the four jets into two W s. Fits with reconstructed W mass outside the range $74 < m_W^{rec} < 88$ GeV/ c^2 were rejected and, of the remaining fits, the one with minimum χ^2 was accepted.

The efficiency of the selection procedure was evaluated from fully simulated events to be $(75.7 \pm 0.2)\%$. A total of 1130 events was selected from data corresponding to an integrated luminosity of 155.4 pb $^{-1}$. Background contributions of 1.26 ± 0.02 pb

and 0.187 ± 0.007 pb were estimated from $q\bar{q}\gamma$ and $jj\ell\nu$ production, respectively. The method used in the data to assign the reconstructed jets to W pairs was applied to a sample of simulated events generated with only the three doubly resonant diagrams for WW production present in the production amplitude; in this model the efficiency of the procedure was estimated to be about 74%.

An additional problem in the analysis of the $jjjj$ state is to distinguish the pair of jets constituting the W^+ decay products from that from the W^- . This ambiguity can be partly resolved by computing jet charges from the momentum-weighted charge of each particle belonging to the jet, $Q_{jet} = \sum_i q_i |p_i|^{0.5} / \sum_i |p_i|^{0.5}$ (where the exponent is chosen empirically), and defining the W^\pm charges, Q_{W^+} and Q_{W^-} , as the sums of the charges of the two daughter jets. Following the method of [9], the distribution of the difference $\Delta Q = Q_{W^-} - Q_{W^+}$ was then used to construct an estimator $P(\Delta Q)$ of the probability that the pair with the more negative value of Q_W is a W^- . An estimate of the efficiency of this procedure was made by flagging all correctly associated jet pairs reconstructed from simulated events with $\Delta Q < 0$ as W^- and comparing with the generated information: a value of 77% was obtained.

Selection of events in the $\ell^+\ell^-X$ topology:¹

Events selected as candidates for the $\ell^+\ell^-X$ final state were required to have exactly two charged particles of the opposite sign, both identified as muons or electrons according to criteria defined in [6]. Both leptons were required to be of the same flavour. The normal track selections were tightened: the track was required to pass within 1 mm of the interaction point in the xy plane (perpendicular to the beam) and within 4 cm in z . Lepton candidates were also required to have momentum below 75 GeV/ c , with transverse component above 20 GeV/ c . Events were rejected if there was an energy deposition of more than 3 GeV in the barrel or forward electromagnetic calorimeters which was not associated with one of the charged particle tracks, or if there was a signal in the hermeticity detectors at an angle of more than 120° to either candidate track. In addition, the angle between the two leptons and the angle between the planes containing each lepton direction and the beam axis were both required to be less than 160° , and the polar angle of the missing momentum was required to satisfy $20^\circ < \theta_{miss} < 160^\circ$. Candidate events were required to have total visible energy less than 150 GeV.

Using these criteria, 6 events were selected in the e^+e^-X topology while 6.58 events were expected for Standard Model values of the gauge boson couplings. Most of the expected signal (5.98 ± 0.38 events) was estimated to come from the $e^+e^-\nu\bar{\nu}$ final state, corresponding to a selection efficiency of 21.8%. Contributions of 0.55 ± 0.12 and 0.05 ± 0.03 events were estimated to come from the $e\tau\nu\nu$ and $\tau\tau\nu\nu$ final states, respectively, with an electron or positron produced in the τ decay. In the $\mu^+\mu^-X$ topology, 11 events were selected, while 11.73 events were expected, with 10.63 ± 0.49 events from $\mu^+\mu^-\nu\bar{\nu}$ (corresponding to a selection efficiency of 40.7%), 1.08 ± 0.16 events from $\mu\tau\nu\nu$ and 0.02 ± 0.02 events from $\tau\tau\nu\nu$. No other processes were estimated to contribute significantly to these samples. The $\ell\tau\nu\nu$ and $\tau\tau\nu\nu$ components of the selected samples may also have a dependence on trilinear gauge boson couplings in their production, and this was taken into account in the subsequent analysis.

¹The use of these data in the determination of the cross-section for WW production is reported elsewhere [10], using somewhat different selection criteria.

Selection of events in the ℓX topology:²

In the selection of candidates for the ℓX final state, events were required to have only one charged particle. Only events in which the particle was clearly identified as a muon were accepted. The same criteria were imposed on candidate muon tracks as are described above in the selection of events in the $\ell^+\ell^- X$ topology.

Imposing these criteria, a sample of 12 events was selected in the μX topology. For Standard Model values of the couplings, 11.13 events were expected, comprising 5.38 ± 0.59 events from $e\mu\nu\nu$ production, 1.8 ± 1.1 events from $e^+e^-\mu^+\mu^-$ production, 0.82 ± 0.33 events from $e\tau\nu\nu$, 0.78 ± 0.12 events from $\mu\mu\nu\nu$, 0.55 ± 0.11 events from $\mu\tau\nu\nu$, and 1.7 ± 0.4 and 0.05 ± 0.03 events from $\mu\mu\gamma$ and $\tau\tau\gamma$ production, respectively. All of these contributions were estimated from simulated samples in which one final state lepton was emitted at less than 11° , and hence went undetected, or, if produced at larger angle, failed the reconstruction procedure. All the contributing channels except the last two listed may also have a dependence on trilinear gauge boson couplings in their production and, as in the case of the $\ell^+\ell^- X$ topology, this was taken into account in the subsequent analysis.

Selection of events in the jjX topology:³

Events were selected as candidates for the jjX topology, in which a lepton is presumed lost in the beam pipe and a neutrino is assumed to be produced, if they had at least 4 charged particles, total visible energy in the event less than 110 GeV, total measured transverse momentum greater than 15 GeV/ c , and invariant mass of detected particles exceeding 45 GeV/ c^2 . All detected particles were then clustered into jets using LUCLUS with $d_{join} = 6.5$ GeV/ c . Events were accepted if they had exactly two jets, with at least 2 charged particles in each jet.

Events from the WW final state, with one W decaying leptonically, were suppressed by rejecting events with identified final state leptons (e or μ) of energy exceeding 12 GeV. In order to suppress the contribution from the $q\bar{q}\gamma$ final state, events were rejected if the two jets were collinear to within 20° or if the angle between the planes containing each jet direction and the beam direction was less than 20° . In addition, events were rejected if the direction of the missing momentum lay within 25° of the beam direction, if the direction of either reconstructed jet lay within 25.8° of the beam direction, or if any charged or neutral track of momentum exceeding 1 GeV/ c was reconstructed within a cone of angle 20° about the direction of the missing momentum.

On the application of these criteria to the data, corresponding to an integrated luminosity of 158 pb⁻¹, 63 events were selected. For Standard Model values of the couplings, a total of 62.0 events are expected, comprising 18.8 ± 0.6 events from the $q\bar{q}e\nu$ final state with the electron or positron lost in the beam pipe, 4.0 ± 0.2 events from $q\bar{q}e\nu$ with the electron or positron elsewhere in the detector, 22.3 ± 0.5 events from $q\bar{q}\tau\nu$, 5.5 ± 0.2 events from $q\bar{q}\mu\nu$, 6.1 ± 0.2 events from $q\bar{q}\nu\nu$, 5.0 ± 0.2 events from $q\bar{q}\gamma$ production, and 0.3 ± 0.2 events from $\gamma\gamma$ interactions. All the processes contributing to the selected sample except $q\bar{q}\gamma$ production and two-photon interactions include diagrams with trilinear gauge couplings, and this was taken into account in the subsequent analysis.

²The determination of the cross-section for $W e \nu$ production from these data is reported elsewhere [11], using somewhat different selection criteria.

³See footnote, above.

Selection of events in the γX topology:

The production of the single photon final state, γX , via a $WW\gamma$ vertex proceeds through the fusion diagram shown in figure 1c, while the dominant process giving rise to this final state, $e^+e^- \rightarrow Z\gamma$, with $Z \rightarrow \nu\bar{\nu}$, involves bremsstrahlung diagrams. The sensitivity of the γX final states to anomalous $WW\gamma$ couplings is therefore greatest when the photon is emitted at high polar angle. Events were selected if they had a single shower in the barrel electromagnetic calorimeter, with $45^\circ < \theta_\gamma < 135^\circ$ and $E_\gamma > 6$ GeV, where θ_γ and E_γ are the polar angle and energy, respectively, of the reconstructed photon. It was also required that no electromagnetic showers were present in the forward electromagnetic calorimeters, and a second shower in the barrel calorimeter was accepted only if it was within 20° of the first one. Cosmic ray events were suppressed by requiring that any signal in the hadronic calorimeter be in the same angular region as the signal in the electromagnetic calorimeter, and that the electromagnetic shower should point towards the beam collision point [12]. Using these criteria, 145 events were selected from data corresponding to an integrated luminosity of 154.7 pb^{-1} , corresponding to an observed cross-section of $(1.80 \pm 0.15 \pm 0.15) \text{ pb}$. The Standard Model expectation is 157.7 ± 3.7 events. Values for the triple gauge boson couplings were fitted in the region $E_\gamma > 50$ GeV, which contained 59% of the events. In this region, an overall selection efficiency of $c.55\%$ was estimated, with negligible background contamination.

Event simulation:

Various Monte Carlo models were used in the calculation of cross-sections as a function of coupling parameters in the different final states analysed. In the study of the $jj\ell\nu$ and $jjjj$ channels, the four-fermion generators EXCALIBUR [13] and ERATO [14] were used, the ℓX , $\ell^+\ell^- X$ and jjX final states used calculations based on the program DELTGC [15], cross-checked with GRC4F [16], and DELTGC and NUNUGPV [17] were used to calculate expected signals in the γX topology. The EXCALIBUR and GRC4F models were interfaced to the JETSET hadronization model [7], tuned to Z data [18], and to the full DELPHI simulation program [5]. The study of backgrounds due to $q\bar{q}(\gamma)$ production was made using fully simulated events from the PYTHIA model [19], while EXCALIBUR was used to study the $qq\nu\nu$ contribution to the jjX topology and KORALZ [20] was used in the calculation of backgrounds in the ℓX final state. PYTHIA and EXCALIBUR were used in the simulation of events from ZZ production. Two-photon backgrounds were studied using the generators of Berends, Daverveldt and Kleiss [21] and with the TWOGAM generator [22].

3 Methods used in the determination of the couplings

Data in both the $jj\ell\nu$ and $jjjj$ channels were analyzed using methods based on that of Optimal Observables [23]. The methods exploit the fact that the differential cross-section, $d\sigma/d\vec{V}$, where \vec{V} represents the phase space variables, is quadratic in the trilinear gauge coupling parameters:

$$\frac{d\sigma(\vec{V}, \vec{\lambda})}{d\vec{V}} = c_0(\vec{V}) + \sum_i c_1^i(\vec{V}) \cdot \lambda_i + \sum_{i \leq j} c_2^{ij}(\vec{V}) \cdot \lambda_i \cdot \lambda_j, \quad (1)$$

where the sums in i, j are over the set $\vec{\lambda} = \{\lambda_1, \dots, \lambda_n\}$ of parameters under consideration. It has been shown that the ‘‘Optimal Variables’’ $c_1^i(\vec{V})/c_0(\vec{V})$ and $c_2^{ij}(\vec{V})/c_0(\vec{V})$, approximated for real data by using the reconstructed phase space variables $\vec{\Omega}$ as arguments of the c_1^i and c_2^{ij} , have the same estimating efficiency as can be obtained in unbinned likelihood fits of parameters λ_i to the data [24].

In the determination of a single parameter λ , the joint distribution of the quantities $c_1(\vec{\Omega})/c_0(\vec{\Omega})$ and $c_2(\vec{\Omega})/c_0(\vec{\Omega})$ was compared with the expected distribution, computed from events generated with EXCALIBUR and passed through the full detector simulation. Extended maximum likelihood fits were made to the binned distribution in these variables, at each stage reweighting [25] the simulated data, which had been generated at a few values of the couplings, to the required value of λ using the matrix element calculation of the ERATO generator [14]. In the case of events in the $jj\ell\nu$ topology, the binning in these two variables was made using a multidimensional clustering technique, described in detail in [26]. This is an economical binning method in which the n_d real data points are used as seeds to divide the phase space into an equal number of multidimensional bins. Each simulated event is associated with the closest real event, resulting in an equiprobable division of the space of the Optimal Variables in which it is assumed that the best available knowledge of the probability density function is that of the real data points themselves.

The use of such a technique becomes of particular importance when simultaneous fits to two coupling parameters are performed. The number of Optimal Variables then increases to five: c_1^1/c_0 , c_1^2/c_0 , c_2^{11}/c_0 , c_2^{22}/c_0 and c_2^{12}/c_0 , and the use of equal sized bins in a space of this number of dimensions is impractical. For events in the $jj\ell\nu$ topology, an extended maximum likelihood fit was performed over the n_d bins for each pair of coupling parameters (λ_1, λ_2) using this method.

A somewhat different technique was used in 2-parameter fits to data in the $jjjj$ topology. In this case, extended maximum likelihood fits were made to the binned joint distribution of only the first order terms c_1^1/c_0 and c_1^2/c_0 in (1), but an iterative procedure was used, at each stage expanding the expression for the differential distribution of the phase space variables \vec{V} about the values $(\tilde{\lambda}_1, \tilde{\lambda}_2)$ obtained in the previous iteration:

$$\frac{d\sigma(\vec{V}, \lambda_1, \lambda_2)}{d\vec{V}} = c_0(\tilde{\lambda}_1, \tilde{\lambda}_2, \vec{V}) + c_1^1(\tilde{\lambda}_1, \tilde{\lambda}_2, \vec{V})(\lambda_1 - \tilde{\lambda}_1) + c_1^2(\tilde{\lambda}_1, \tilde{\lambda}_2, \vec{V})(\lambda_2 - \tilde{\lambda}_2) + \dots \quad (2)$$

It has been shown in reference [24] that when this iterative procedure has converged sufficiently, the first order terms retain the whole sensitivity of the Optimal Variables to the coupling parameters $\vec{\lambda}$, the contribution from the higher order terms becoming negligible. In practice, this was achieved after about three or four iterations.

In both the $jj\ell\nu$ and $jjjj$ channels, an additional analysis was performed using more directly measured kinematic variables in order to corroborate results obtained from the methods described above. For events in the $jj\ell\nu$ topology, a binned maximum likelihood fit was made to the joint distribution in $\cos\theta_W$, the W^- production angle, and $\cos\theta_\ell$, the polar angle of the produced lepton with respect to the incoming e^\pm of the same sign. In this study, somewhat looser criteria were imposed in the selection of the events,

giving a total sample of 885 semileptonic events, with estimated efficiencies of 84%, 71% and 48% for muon, electron and tau events, respectively, and an estimated background contamination of 1.0 pb. A 4-constraint kinematic fit was then applied to the events, requiring conservation of four-momentum, and the variables $\cos \theta_W$ and $\cos \theta_\ell$ computed from the fitted four-vectors. The expected number of events in each bin was estimated using events generated with PYTHIA corresponding to the reaction $e^+e^- \rightarrow W^+W^-$ and passed through the full detector simulation procedure. Again, a reweighting technique was used to determine the expected number of events for given values of the coupling parameters.

In the $jjjj$ topology, the second analysis involved a binned extended maximum likelihood fit to the production angular distribution. Events were selected by constructing a probability function from the distributions of several kinematic variables, namely: the value of d_{join} in the LUCLUS algorithm when four rather than three natural jets are reconstructed, the sphericity, the angle between the two fastest reconstructed jets, the minimal multiplicity in a jet, the second Fox-Wolfram moment, the D variable (defined above), s' (defined above), the fitted W masses, the product of the energy ratios of the two jets in the two reconstructed dijets, the minimal transverse momentum with respect to the beam axis of the 15 most energetic tracks in the event, and the transverse momentum of the jet pair obtained by forcing the reconstruction of exactly two jets. Using this procedure, a sample of 1331 events was selected with estimated efficiency of $(86.6 \pm 0.2)\%$ and purity of $(74.4 \pm 0.4)\%$. As in the case of the previously described analysis of this channel, momentum-weighted jet charges were then calculated to try to distinguish the W^+ decay products from those of the W^- , and a folded production angle, $P_{W^+}(\Delta Q) \cos \theta_W - (1 - P_{W^-}(\Delta Q)) \cos \theta_W$, was used in the construction of the angular distribution. The experimental distribution was compared with predictions obtained from events generated with PYTHIA, passed through the full detector simulation procedure, and reweighted in the fit for given values of the coupling parameters.

The analysis procedures described above are similar to those used in our previously reported analysis of data at 183 GeV, though somewhat different applications of the method of Optimal Observables were used there in the analyses of the $jj\ell\nu$ and $jjjj$ final states.

Data in the topologies ℓX and $\ell^+\ell^-X$ were analysed using maximum likelihood fits to the observed total numbers of events selected, while data in the jjX topology were fitted using a binned extended maximum likelihood fit to the distribution of $\cos \theta_{jj}$, the angle between the two reconstructed jets. The γX data were fitted using a binned extended maximum likelihood fit to the distribution of the reconstructed photon energy, E_γ , in the region $E_\gamma > 50$ GeV, which has the maximum sensitivity to anomalous triple gauge boson couplings.

4 Results on WWV and ZZV couplings

The results obtained for the triple gauge boson couplings from the data in each of the final states and using the methods discussed above are shown in table 1. Values for the couplings Δg_1^Z , $\Delta \kappa_\gamma$ and λ_γ at the WWV vertex are given in table 1a, and those for the couplings f_4^γ , f_4^Z , f_5^γ and f_5^Z at the ZZV vertex in table 1b. The results for the ZZV couplings are given from combined data in the jjX and $\ell^+\ell^-X$ topologies; in this

combination the dominant contribution to the precision is from the jjX topology. The results from all topologies are combined with those previously analysed by DELPHI at 183 GeV and reported in reference [4] to give the values of the coupling parameters, their 1 s.d. errors and the 95% confidence limits shown in table 2. In the combination, the results in the $jj\ell\nu$ and $jjjj$ topologies from the methods based on Optimal Observables were used, as these use all the available kinematic information and hence are expected to have the greatest precision. In the fit to each coupling parameter, the values of the other parameters were held at zero, their Standard Model values. The results of fits in which two parameters were allowed to vary are shown in figure 2. In no case is any deviation seen from the Standard Model prediction of zero for the couplings determined.

The systematic errors shown in table 1 and included in the results shown in table 2 contain contributions from the effects estimated to be of the greatest importance in each of the analyses listed. In particular, the effect of limited Monte Carlo statistics in the evaluation of signal efficiencies and of background contaminations are included in each case. Other possible sources of systematic error, including effects of the event reconstruction procedure, of uncertainties in the jet hadronization models used and, in the $jjjj$ final state, of colour reconnection effects, have not been considered in the present analysis.

5 Conclusions

Values for the WWV couplings Δg_1^Z , $\Delta\kappa_\gamma$ and λ_γ have been derived from a preliminary analysis of DELPHI data at 189 GeV. The results have been combined with previously published values from DELPHI data at lower energies, giving an overall improvement in precision by a factor of about two over that of the 183 GeV data [4]. In addition, data from channels to which processes containing a ZZV vertex can contribute have been used to derive preliminary values for the neutral trilinear gauge boson coupling parameters f_4^γ , f_4^Z , f_5^γ and f_5^Z .

There is no evidence for deviations from Standard Model predictions in any of the couplings studied.

References

- [1] K. Hagiwara, R. Peccei, D. Zeppenfeld and K. Hikasa, Nucl. Phys. **B282** (1987) 253.
- [2] G. Gounaris, J.-L. Kneur and D. Zeppenfeld, in *Physics at LEP2*, eds. G. Altarelli, T. Sjöstrand and F. Zwirner, CERN 96-01 Vol.1, 525 (1996).
- [3] DELPHI Collaboration, P. Abreu *et al.*, Phys. Lett. **B423** (1998) 194.
- [4] DELPHI Collaboration, P. Abreu *et al.*, *Measurements of the Trilinear Gauge Boson Couplings $WWV(V \equiv \gamma, Z)$ in e^+e^- Collisions at 183 GeV*, CERN-EP/99-62 (1999), submitted to Phys. Lett. **B**.
- [5] DELPHI Collaboration, P. Aarnio *et al.*, Nucl. Inst. Meth. **A303** (1991) 233, DELPHI Collaboration, P. Abreu *et al.*, Nucl. Inst. Meth. **A378** (1996) 57.
- [6] DELPHI Collaboration, P. Abreu *et al.*, E. Phys. J. **C2** (1998) 581.

- [7] T. Sjöstrand, *PYTHIA 5.7 / JETSET 7.4*, CERN-TH.7112/93 (1993).
- [8] P. Abreu *et al.*, Nucl. Inst. Meth. **A427** (1999) 487.
- [9] ALEPH Collaboration, R. Barate *et al.*, Phys. Lett. **B422** (1998) 369.
- [10] P. Buschmann *et al.*, DELPHI Collaboration, *Measurement of the W-pair production cross-section and W branching ratios at $\sqrt{s} = 189$ GeV*, Abstract 6-78, contributed to the HEP'99 Conference, Tampere, Finland, (1999).
- [11] DELPHI Collaboration, *Measurement of the single-W production cross-section at LEP2*, Abstract 6-381, contributed to the HEP'99 Conference, Tampere, Finland, (1999).
- [12] DELPHI Collaboration, *Analysis of the single photon channel at LEP 2*, Abstract 206, contributed to ICHEP98, Vancouver, (1998).
- [13] F.A. Berends, R. Kleiss and R. Pittau, *EXCALIBUR*, in *Physics at LEP2*, eds. G. Altarelli, T. Sjöstrand and F. Zwirner, CERN 96-01 Vol.2, 23 (1996).
- [14] C.G. Papadopoulos, Comp. Phys. Comm. **101** (1997) 183.
- [15] O. Yushchenko, *DELTC: A program for four-fermion calculations*, DELPHI note DELPHI 99-4 PHYS 816 (1999).
- [16] J. Fujimoto *et al.*, *GRC4F*, in *Physics at LEP2*, eds. G. Altarelli, T. Sjöstrand and F. Zwirner, CERN 96-01 Vol.2, 23 (1996).
- [17] G. Montagna *et al.* Nucl. Phys. **B452** (1995) 161.
- [18] DELPHI Collaboration, P. Abreu *et al.*, Z. Phys. **C73** (1996) 11.
- [19] T. Sjöstrand, *PYTHIA 5.719 / JETSET 7.4*, in *Physics at LEP2*, eds. G. Altarelli, T. Sjöstrand and F. Zwirner, CERN 96-01 Vol.2, 41 (1996).
- [20] S. Jadach, B.F.L Ward and Z. Was, Comp. Phys. Comm. **79** (1994) 503.
- [21] F.A. Berends, P.H. Daverveldt and R. Kleiss, Comp. Phys. Comm. **40** (1980) 271, 285 and 309.
- [22] S. Nova, S. Olchevski and T. Todorov, in *Physics at LEP2*, eds. G. Altarelli, T. Sjöstrand and F. Zwirner, CERN 96-01 Vol.2, 224 (1996).
- [23] M. Diehl and O. Nachtmann, Z. Phys. **C62** (1994) 397.
- [24] G.K. Fanourakis, D. Fassouliotis and S.E. Tzamarias, Nucl. Inst. Meth. **A414** (1998) 399;
G.K. Fanourakis, D. Fassouliotis, A. Leisos, N. Mastrogiannopoulos and S.E. Tzamarias, *Extended Modified Observable technique for a Multi-Parametric Trilinear Gauge Coupling Estimation at LEP II*, hep-ex/9812002 (1998), to be published in Nucl. Inst. Meth. **A**.

- [25] G.K. Fanourakis, D.A. Fassouliotis and S.E. Tzamarias, Nucl. Inst. Meth. **A412** (1998) 465.
- [26] G.K. Fanourakis *et al.*, *Multidimensional Binning Techniques for a Two Parameter Trilinear Gauge Coupling Estimation at LEP II*, hep-ex/9812001 (1998), to be published in Nucl. Inst. Meth. **A**.

a)	Δg_1^Z	$\Delta \kappa_\gamma$	λ_γ	
$jj\ell\nu$ (Optimal Variables)	$0.02_{-0.08}^{+0.08} \pm 0.02$	$0.34_{-0.26}^{+0.28} \pm 0.09$	$0.06_{-0.09}^{+0.09} \pm 0.02$	
$jj\ell\nu$ ($\cos\theta_W, \cos\theta_\ell$)	$-0.04_{-0.11}^{+0.12} \pm 0.03$	$0.00_{-0.28}^{+0.48} \pm 0.10$	$0.01_{-0.13}^{+0.15} \pm 0.03$	
$jjjj$ (Optimal Variables)	$-0.09_{-0.12}^{+0.14} \pm 0.06$	$0.12_{-0.31}^{+0.54} \pm 0.20$	$0.01_{-0.15}^{+0.17} \pm 0.04$	
$jjjj$ ($\cos\theta_W$)	$-0.07_{-0.13}^{+0.17} \pm 0.06$	$0.06_{-0.31}^{+0.57} \pm 0.23$	$-0.05_{-0.15}^{+0.19} \pm 0.06$	
$\ell^+\ell^-X$	$0.03_{-0.74}^{+0.74} \pm 0.002$	$0.36_{-1.65}^{+1.69} \pm 0.23$	$0.04_{-0.82}^{+0.83} \pm 0.003$	
ℓX	$1.24_{-4.50}^{+1.77} \pm 1.20$	$0.14_{-0.68}^{+0.48} \pm 0.25$	$0.63_{-2.22}^{+0.80} \pm 0.57$	
jjX	$0.20_{-0.75}^{+0.54} \pm 0.16$	$0.25_{-0.38}^{+0.28} \pm 0.08$	$0.53_{-1.14}^{+0.31} \pm 0.09$	
γX	–	$0.70_{-0.99}^{+0.77} \pm 0.15$	$0.65_{-1.79}^{+1.03} \pm 0.25$	
b)	f_4^γ	f_4^Z	f_5^γ	f_5^Z
$jjX + \ell^+\ell^-X$	$0.01_{-1.04}^{+1.03} \pm 0.04$	$-0.00_{-1.74}^{+1.74} \pm 0.02$	$-1.45_{-1.40}^{+4.29} \pm 0.52$	$-3.19_{-2.18}^{+6.63} \pm 0.72$

Table 1: Fitted values a) of WWV couplings, b) of ZZV couplings, from DELPHI data at 189 GeV using the methods described in the text. The first errors given for each value are the 1 s.d. statistical errors; the second is the systematic error. In the fits to each coupling parameter, the other couplings were set to their Standard Model values.

Coupling parameter	Fitted value	95% confidence interval
Δg_1^Z	$-0.02_{-0.06}^{+0.07}$	$-0.14, 0.11$
$\Delta \kappa_\gamma$	$0.23_{-0.16}^{+0.16}$	$-0.08, 0.55$
λ_γ	$0.02_{-0.08}^{+0.08}$	$-0.14, 0.19$
f_4^γ	$0.01_{-1.04}^{+1.03}$	$-1.59, 1.58$
f_4^Z	$-0.00_{-1.74}^{+1.74}$	$-2.67, 2.67$
f_5^γ	$-1.45_{-1.49}^{+4.32}$	$-3.90, 3.87$
f_5^Z	$-3.19_{-2.30}^{+6.67}$	$-7.09, 5.71$

Table 2: Values of triple gauge boson couplings combining DELPHI data from various sources, as described in the text. The second column shows the value of each coupling corresponding to the minimum of the combined negative log-likelihood distribution and its 1 s.d. errors. The third column shows the 95% confidence intervals on the parameter values. Both the statistical errors and independent systematic errors are included. In the fits to each coupling parameter, the other two couplings were set to their Standard Model values.

DELPHI preliminary

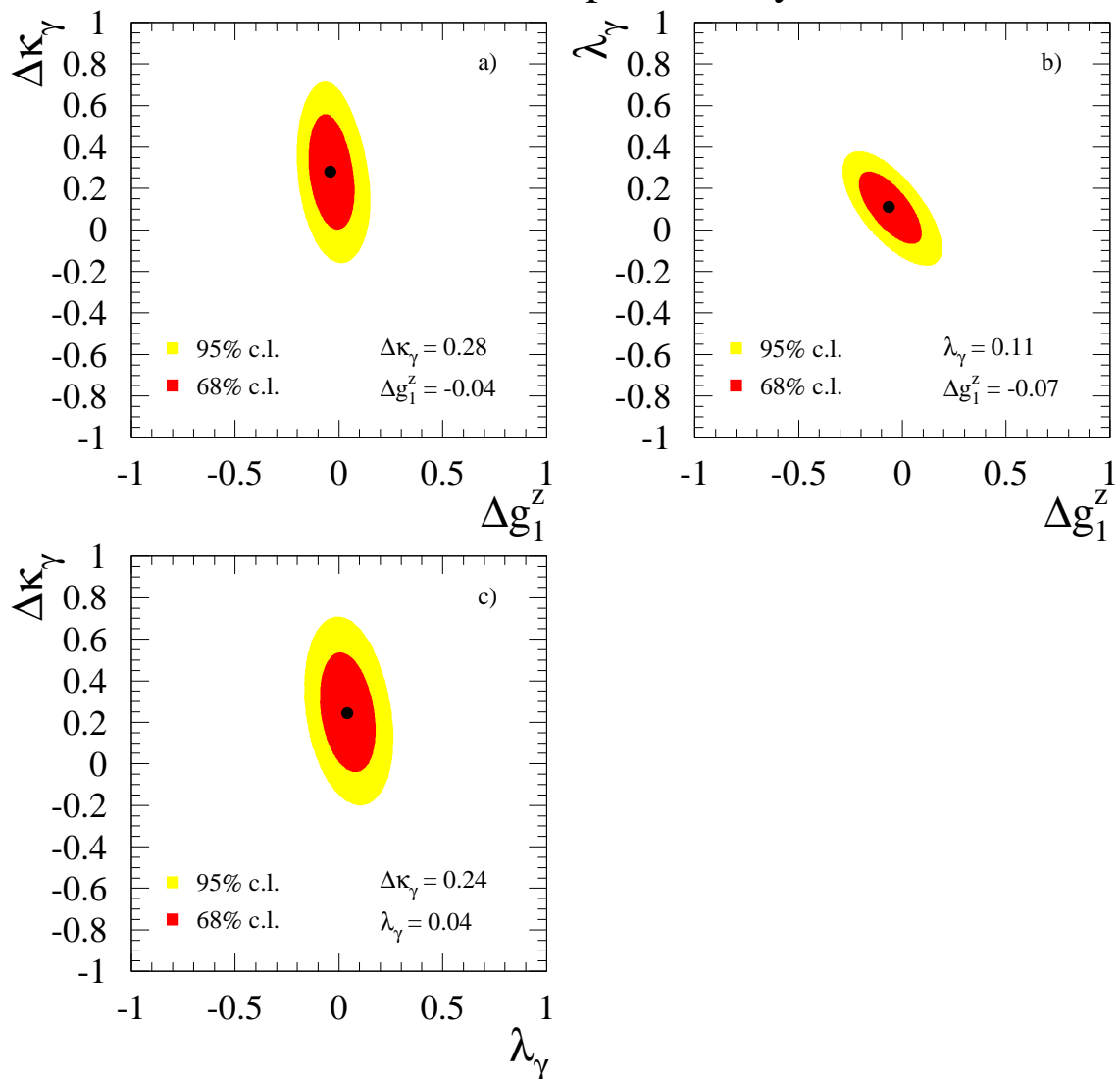


Figure 2: Results of fits in the planes of the parameters a) $(\Delta\kappa_\gamma, \Delta g_1^Z)$, b) $(\lambda_\gamma, \Delta g_1^Z)$ and c) $(\Delta\kappa_\gamma, \lambda_\gamma)$ using data from the final states listed in table 1 combined with DELPHI results at lower energy [4]. In the combination, the analyses of the $jj\ell\nu$ and $jjjj$ final states based on Optimal Observable techniques were used. In each case the third parameter was fixed at its Standard Model value. The values maximizing the likelihood function and the regions accepted at the 68% and 95% confidence levels are shown.